

Approximate Projections onto the Positive Semidefinite Cone Using Randomization

Morgan Jones^{*} James Anderson[†]

Abstract

This paper presents two novel algorithms for approximately projecting symmetric matrices onto the Positive Semidefinite (PSD) cone using Randomized Numerical Linear Algebra (RNLA). Classical PSD projection methods rely on full-rank deterministic eigen-decomposition, which can be computationally prohibitive for large-scale problems. Our approach leverages RNLA to construct low-rank matrix approximations before projection, significantly reducing the required numerical resources. The first algorithm utilizes random sampling to generate a low-rank approximation, followed by a standard eigen-decomposition on this smaller matrix. The second algorithm enhances this process by introducing a scaling approach that aligns the leading-order singular values with the positive eigenvalues, ensuring that the low-rank approximation captures the essential information about the positive eigenvalues for PSD projection. Both methods offer a trade-off between accuracy and computational speed, supported by probabilistic error bounds. To further demonstrate the practical benefits of our approach, we integrate the randomized projection methods into a first-order Semi-Definite Programming (SDP) solver. Numerical experiments, including those on SDPs derived from Sum-of-Squares (SOS) programming problems, validate the effectiveness of our method, especially for problems that are infeasible with traditional deterministic methods.

^{*}M. Jones is with the School of Electrical and Electronic Engineering, The University of Sheffield. E-mail: morgan.jones@sheffield.ac.uk

[†]J. Anderson is with Department of Electrical Engineering, Columbia University . E-mail: anderson@ee.columbia.edu

1 Introduction

Square symmetric matrices whose eigenvalues are non-negative are called Positive semidefinite (PSD) matrices and play a pivotal role in many areas of scientific computing. They arise naturally in applications such as *semidefinite programming* (SDP) [1], statistical inference [2], solutions to Lyapunov equations [3], and Hessians of functions [4]. PSD matrices possess specialized factorization schemes that are often more efficient than their non-PSD counterparts, the highly stable Cholesky decomposition [5] being one such example. Often, a matrix that is known to be PSD, such as a correlation matrix [2], is estimated from data and as a result is not exactly PSD but rather “almost” PSD. Therefore, the task of finding the closest PSD matrix, or equivalently projecting a matrix onto the PSD cone, is a fundamental computation in numerical linear algebra. Unfortunately, existing algorithms for computing such projections scale poorly with the matrix dimension, making them impractical for large-scale problems. To address this limitation, in this paper we provide methods that trade off accuracy for efficiency by employing techniques from randomized numerical linear algebra to compute approximate PSD projections.

The problem of projecting a symmetric matrix $X \in \mathbb{R}^{n \times n}$ onto the PSD cone can be formulated as the convex optimization problem: $\min_{Y \succeq 0} \|X - Y\|_2^2$. This problem has a closed form solution: compute the eigen-decomposition of X , zero out the negative eigenvalues, and re-multiply the modified factors to yield the projected matrix. For a dense $n \times n$ matrix, this demands $\mathcal{O}(n^3)$ floating-point operations (FLOPs), making it impractical for large n . Moreover, directly solving the aforementioned optimization problem as a SDP problem, is also intractable for large n as the positive semidefinite constraint, although convex, is expensive to encode. Second order interior point methods provide the most accurate solutions to this type of problem. In [6] the authors argue that the per-iteration complexity of a naive interior point method is of the order n^6 , but, when accounting for structure in specific problems, this can be reduced to n^3 . Alternatively, first-order methods such as those used in [7, 8, 9, 10] exhibit slower convergence but require less memory and computation at each iteration. Yet during each iteration, a projection onto the PSD cone is required and as noted in [11], “this projection operation typically takes the majority of solution time, sometimes 90% or more”.

Existing approximate PSD projection methods, such as [12] and [5], also entail $\mathcal{O}(n^3)$ FLOPs. In this work, we are concerned with use cases where n is sufficiently large that a cubic dependence is intractable. We use Randomized Numerical Linear Algebra (RNLA) [13] for computing approximate low-rank pro-

jections onto the PSD cone. Our method of using low rank approximations to construct approximate PSD projections is justified by the pervasiveness of low rank matrices appearing in practical applications and data science as a whole [14]. Using RNLA, we demonstrate the possibility of computing inexact PSD projections with $\mathcal{O}(kn^2)$ FLOPs, where $k \ll n$ is a user-defined parameter that can be increased to improve accuracy. At little extra computational cost, we introduce a scaling method that biases the RNLA algorithm to construct a low-rank matrix approximation focused on capturing information about the positive eigenvalues, rather than the leading singular values. We demonstrate that in some cases, this approach yields a better PSD projection approximation. This improvement arises because the method reduces computational effort spent on capturing information on large negative eigenvalues, which are inevitably set to zero in the PSD projection.

Randomization has previously been employed in [15] for relaxing SDPs to linear programs via eigenvalue approximations, and also in [16] to relax SDPs to smaller SDPs. Our use of randomization is independent to SDPs, instead, we employ randomness for direct PSD cone projection, allowing for seamless integration into existing first-order SDP solvers. Our proposed method is more similar to the works of [17, 11, 18] that each solve SDPs via approximate PSD projections. In [17], an approximate PSD projection based Jacobi’s method showed impressive performance but degraded significantly with larger matrices. On the other hand, both [11] and [18] base their projection on the Krylov method that is known to suffer from inherent numerical instability issues [13]. Furthermore, Krylov methods need multiple passes over the matrix, a computational bottleneck for large matrices not fitting in fast memory, while RNLA methods require just a single pass. Surprisingly, RNLA-based methods have only recently been applied to numerical problems in control [19, 20, 21].

To demonstrate the effectiveness of using our proposed RNLA PSD projection in first order SDP solvers we have implemented our approximate projections in a method based on [22]. Although [22] dealt with the problem of finding feasible solutions to SDP problems it is fairly straight forward to modify this method to solve general SDP problems. This approach can be simply interpreted as Gradient Descent (GD) on the convex and coercive Lagrangian of the regularized SDP. Each iteration of GD requires the evaluation of the gradient which in this setting involves the computation of a PSD projection. Hence, rather than computing the exact gradient we compute approximate gradients using our RNLA PSD projection. We provide a bound on the gradient approximation error that can be used together with the existing convergence results for problems involving stochastic

biased gradient errors, as discussed in the literature [23, 24, 25]. We apply our first order GD algorithm with randomized gradient error to several problems, including randomly generated SDPs and SDPs resulting from Sum-of-Square (SOS) problems.

2 Notation

Denote the set of symmetric matrices by \mathbb{S}_n and the set of symmetric positive semidefinite matrices by \mathbb{S}_n^+ . We often use $A \succcurlyeq 0$ to denote $A \in \mathbb{S}_n^+$, and $A \succcurlyeq B$ to denote $A - B \in \mathbb{S}_n^+$. For $A \in \mathbb{S}_n^+$, $\sqrt{A} \in \mathbb{S}_n^+$ is defined such that $\sqrt{A}^\top \sqrt{A} = \sqrt{A} \sqrt{A} = A$ (note that the square root of a matrix, defined in this way, is unique [26]). We also use $A^{\frac{1}{2}}$ in place of \sqrt{A} . For $A \in \mathbb{S}_n$, we index the eigenvalues of A in increasing order by $\lambda_1(A) \geq \dots \geq \lambda_n(A)$ and the singular values by $\sigma_1(A) \geq \dots \geq \sigma_n(A)$. We denote the Schatten p -norms for $A \in \mathbb{S}_n$ as $\|A\|_p = (\sum_{i=1}^n \sigma_i(A)^p)^{\frac{1}{p}}$. In particular, the Frobenius norm and spectral norm of A are denoted by $\|A\|_2 = \sqrt{\text{Tr}(A^\top A)} = \sqrt{\sum_{i=1}^n \sigma_i(A)^2}$ and $\|A\|_\infty = \max_{1 \leq i \leq n} \sigma_i(A) = \sigma_1(A)$ under our p -norm notation. When it is not important which norm is used we simply use $\|\cdot\|$. We denote $D = \text{diag}(\lambda_1, \dots, \lambda_n)$ to mean that $D \in \mathbb{R}^{n \times n}$ is a diagonal matrix such that $D_{i,i} = \lambda_i$ and $D_{i,j} = 0$ for $i \neq j$. Moreover, for $D = \text{diag}(\lambda_1, \dots, \lambda_n)$ we denote $\max(D, \beta) := \text{diag}(\max\{\lambda_1, \beta\}, \dots, \max\{\lambda_n, \beta\})$ and $D_+ := \max(D, 0)$. We denote the row vector of ones by $\mathbf{1}_n = [1, \dots, 1] \in \mathbb{R}^{1 \times n}$.

3 Projecting onto the PSD Cone

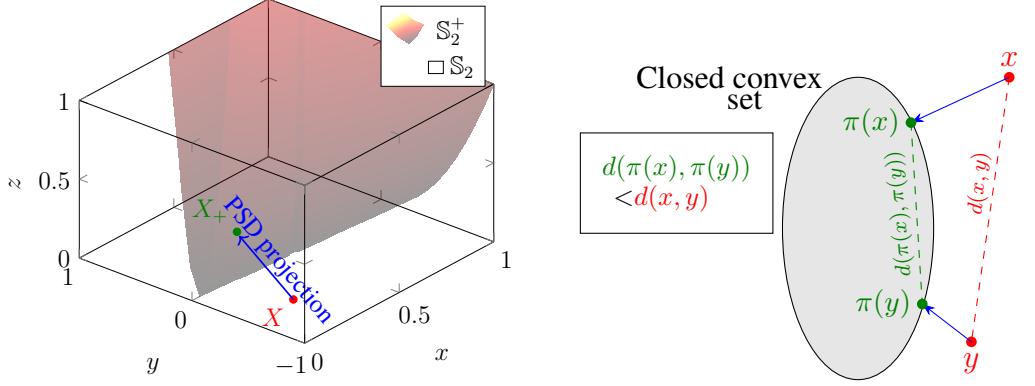
Let us now consider the problem of projecting a given matrix $X \in \mathbb{S}_n$ onto \mathbb{S}_n^+ , i.e., finding the closest element in \mathbb{S}_n^+ to $X \in \mathbb{S}_n$. This task can be formulated as the optimization problem:

$$X_+ := \arg \min_{Y \in \mathbb{S}_n^+} \|X - Y\|_2^2. \quad (1)$$

The solution to Opt. (1) is described in the theorem below:

Theorem 1 (Page 399 [27]). *Consider $X \in \mathbb{S}_n$. Then there is a unique solution to the optimization problem given in Equation (1) given by*

$$X_+ = U D_+ U^\top, \quad (2)$$



(a) For a symmetric matrix $X = \begin{bmatrix} x & y \\ y & z \end{bmatrix}$ the PSD cone, \mathbb{S}_2^+ , can be characterized as the set of matrix element points obeying $z \geq 0$, $x \geq 0$ and $xz \geq y^2$ by ensuring the leading principal minors are nonnegative.

(b) The non-expansive property of projections onto closed convex sets in \mathbb{R}^n .

Figure 1: Projection descriptions and properties.

where $X = UDU^\top$ is the eigen-decomposition of $X \in \mathbb{S}_n$.

Theorem 1 (visualized in Fig. 1a) shows that finding projections onto the PSD cone by solving Opt. (1) numerically boils down to computing eigenvalue decompositions, an operation that requires $\mathcal{O}(n^3)$ floating point operations (flops). For large $n \in \mathbb{N}$ this cost becomes prohibitive. We next propose a method that approximately computes projections at a cost of $\mathcal{O}(kn^2)$, where $k \ll n$ is a user chosen parameter that can be increased to reduce approximation error.

3.0.1 Low-Rank Randomized PSD Projection

Techniques from randomized numerical linear algebra (RNLA) offer an efficient and scalable alternative to classical deterministic numerical linear algebra algorithms. Surprisingly, RNLA approaches are often more robust than their deterministic counterparts. Moreover, they are often easily parallelizable.

We follow the RNLA-based approach of [13] to approximate the range of a given matrix by a low(er) dimensional subspace. More concretely, we seek to find a matrix $Q \in \mathbb{R}^{n \times k}$ with orthonormal columns where $Q^\top Q = I$, and $k < n$ such that $X \approx QQ^\top X$, where \approx should be interpreted as

$$\|(I - QQ^\top)X\| \leq \epsilon, \quad (3)$$

for some user-specified tolerance $\epsilon \geq 0$ (clearly $QQ^\top \neq I$). The fewer columns there are in Q the larger the computational saving. Following [13], Q can be found via random sampling (at a cost proportional to the cost of a matrix-vector multiplication) and an economy QR decomposition of an $n \times k$ matrix.

Specifically, to find $Q \in \mathbb{R}^{n \times k}$ we sample the range of X by drawing an n -dimensional random¹ test vector ω_i and computing $y_i = X\omega_i$. Sampling k times and writing in matrix notation gives $Y = X\Omega$ where $\Omega = [\omega_1, \dots, \omega_k]$. The intuition behind randomized algorithms is that the span of the column space of X is approximately the span of the column space of Y , thus an exact basis for the range of Y should provide a good approximation for the basis of X . The range of Y is a subspace of dimension k which can be cheaply computed using a standard economic QR decomposition, obtaining $Q \in \mathbb{R}^{n \times k}$. If X has an approximately rank- k structure then Eq. (3) holds. In practice, if a rank- k approximation to X is sought, then $k + l$ random sample are obtained. Typically $l = 10$ works very well in practice [13]. It is well known that low-rank approximations perform best when the singular values decay rapidly. For matrices with slow spectral decay, one can instead employ the power iteration method and work with the matrix $W = (XX^\top)^q X$ with q a small integer instead of X [28]. Intuitively, W and X have the same singular vectors, however, the singular values of W that are less than one are compressed towards zero. The steps above are formalized as an algorithm referred to as the *randomized range finder* that is recalled from [13] in Algorithm 1.

Algorithm 1 Randomized Range Finder [13, p.244].

Function $Q = \text{range_finder}(X, k, l, q)$.

Input: $X \in \mathbb{R}^{m \times n}$, $k, l, q \in \mathbb{N}$.

Output: $Q \in \mathbb{R}^{n \times (k+l)}$.

- 1: $\Omega = \text{randn}(m, k + l)$
 - 2: $Q = \text{orth}((XX^\top)^q X \Omega)$ $\triangleright [Q, \sim] = \text{QR}((XX^\top)^q X \Omega, \text{'econ'})$
-

For a symmetric matrix, X , we use the approximation $X \approx QQ^\top X QQ^\top$ rather than $X \approx QQ^\top X$. This form preserves symmetry, allowing us to perform

¹The distribution of the test vectors ω_i is not critical. For simplicity vectors with each element drawn iid from $\mathcal{N}(0, 1)$ will suffice and indeed this choice of distribution provides the theoretical results included in this work. However, sparse random vectors such as *subsampled random Fourier transform* (SRFT vectors) offer improved computational performance at the expense of more involved error bounds.

the approximate eigen-decomposition required by our method for computing approximate PSD projections. The approximation $X \approx QQ^\top XQQ^\top$ can be understood as a simultaneous projection onto subsets of both the row and column spaces of X , which are identical for symmetric matrices and hence will have the same projection matrix Q . The following result bounds the difference between the original matrix and its approximate projection $QQ^\top XQQ^\top$, where Q satisfies Eq. (3).

Lemma 1. *Consider $X \in \mathbb{S}_n$ and $Q \in \mathbb{R}^{n \times k}$. Suppose $Q^\top Q = I$, $\|(I - QQ^\top)X\|_\infty \leq \varepsilon_1$ and $\|(I - QQ^\top)X\|_2 \leq \varepsilon_2$ then*

$$\|X - QQ^\top XQQ^\top\|_\infty \leq 2\varepsilon_1 \quad (4)$$

$$\|X - QQ^\top XQQ^\top\|_2 \leq (1 + \sqrt{k})\varepsilon_2 \quad (5)$$

Proof. Under any Schatten norm, using the triangle inequality, the sub-multiplication property and the fact that $\|A^\top\| = \|A\|$, it is easy to show that

$$\begin{aligned} \|X - QQ^\top XQQ^\top\| &\leq \|X - QQ^\top X + QQ^\top X - QQ^\top XQQ^\top\| \\ &\leq \|X - QQ^\top X\| + \|QQ^\top(X - XQQ^\top)\| \leq (1 + \|QQ^\top\|)\|(I - QQ^\top)X\|. \end{aligned} \quad (6)$$

Since $Q \in \mathbb{R}^{n \times k}$ it follows $\text{rank}(QQ^\top) \leq k$. Moreover, since QQ^\top is a symmetric real matrix it has an eigenvalue decomposition, because $Q^\top Q = I$ it follows that,

$$\begin{aligned} \lambda_i(QQ^\top)^2 &= (QQ^\top v_i)^\top QQ^\top v_i = v_i^\top QQ^\top QQ^\top v_i \\ &= v_i^\top QQ^\top v_i = \lambda_i(QQ^\top) \implies \lambda_i(QQ^\top) = 0 \text{ or } 1, \end{aligned} \quad (7)$$

where $v_i \in \mathbb{R}^n$ is the normalized eigenvector associated with eigenvalue $\lambda_i(QQ^\top)$. Hence,

$$\|QQ^\top\|_\infty = \sigma_1(X) \leq 1, \quad (8)$$

$$\|QQ^\top\|_2 = \sqrt{\sum_{i=1}^n \lambda_i(QQ^\top)^2} \leq \sqrt{k}. \quad (9)$$

Eq. (4) follows from Eqs (6) and (8). Eq. (5) follows from Eqs (6) and (9). \square

Using $X \approx QQ^\top XQQ^\top$ we can cheaply compute an approximate eigen-decomposition of $X \in \mathbb{S}_n$ by finding an eigen-decomposition of the symmetric

k -rank matrix $Q^\top X Q = \hat{V} \hat{D} \hat{V}^\top \in \mathbb{S}_k$ with only $\mathcal{O}(kn^2)$ flops.² By setting $\hat{U} = Q \hat{V}$ it follows by Eq. (6) that $X \approx [\hat{U} \ I] \begin{bmatrix} \hat{D} & 0 \\ 0 & 0 \end{bmatrix} \begin{bmatrix} \hat{U}^\top \\ I \end{bmatrix} = \hat{U} \hat{D} \hat{U}^\top$. We then can construct an approximate PSD projection $\hat{X}_+ := \hat{U} \hat{D}_+ \hat{U}^\top \in \mathbb{S}_n^+$. This method for approximate PSD projection is made explicit in Alg. 2.

Algorithm 2 Randomized PSD Projection

Function $\hat{X}_+ = \text{ran_proj}(X, k, l, q)$.

Input: $X \in \mathbb{S}_n, k \in \mathbb{N}, l \in \mathbb{N}$.

Output: $\hat{X}_+ \in \mathbb{S}_n^+$.

1: $Q = \text{range_finder}(X, k, l, q)$

2: $[U, D] = \text{eig}(Q^\top X Q)$

3: $\hat{X}_+ = Q U D_+ U^\top Q^\top$

▷ Algorithm 1

▷ $Q^\top X Q = U D U^\top$

We now provide an error bound on the quality of the approximate PSD projection resulting from Alg. 2. To derive this error bound, we establish Lipschitz-like bounds of a projection using the Frobenius and spectral norms. We will see that in the case of the Frobenius norm, the PSD projection bound presented later in Eq. (10), is a matrix analogue of the well-established non-expansive property of projections onto closed convex subsets of \mathbb{R}^n depicted in Fig 1b (see Prop. 3.1.3 in [29]). This analogue result arises from the isomorphism between the space of symmetric matrices, \mathbb{S}_n , and the Euclidean space $\mathbb{R}^{n(n+1)/2}$ (illustrated for \mathbb{S}_2 in Fig. 1a). Consequently, we can extend the non-expansive property of projections in Euclidean spaces to derive a matrix analogue for the Frobenius norm. However, we will see that this non-expansive property does not hold in general for all matrix norms. In particular it does not hold for the spectral norm as demonstrated in Figure 2. Instead we provide two bounds for the difference in PSD projections under the spectral radius. The first bound, given in Eq. (11), involves a constant that grows with the dimension of the matrices involved, whereas the second bound, given in Eq. (12), provides an expansion constant involving the magnitudes of the matrices involved.

Proposition 1 (PSD projection bounds). *Consider symmetric matrices $X, Y \in$*

²If $X \in \mathbb{S}_n^+$, then the Nystrom method can be used to construct a low rank approximation. However, it will often be the case that $X \notin \mathbb{S}_n^+$.

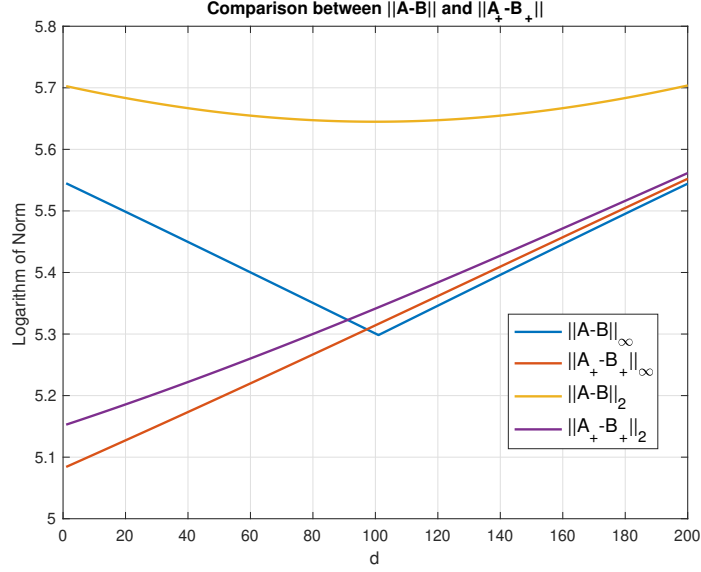


Figure 2: Comparing $\|A - B\|$, $\|A_+ - B_+\|$ where $A = \text{diag}[1, 100]$ and $B = \begin{bmatrix} 0 & 200 \\ 200 & d \end{bmatrix}$ and d is varied between $[0, 200]$. Here, PSD projections are calculated using Eq. (2), where the eigen-decomposition is calculated using Matlab's `eig` function. It is clear that $\|A_+ - B_+\|_2 \leq \|A - B\|_2$ but this is not the case with the spectral norm, $\|A_+ - B_+\|_\infty \not\leq \|A - B\|_\infty$.

\mathbb{S}_n . Then the following inequalities hold,

$$\|X_+ - Y_+\|_2 \leq \|X - Y\|_2. \quad (10)$$

$$\|X_+ - Y_+\|_\infty \leq \frac{1}{2} (\sqrt{n} + 1) \|X - Y\|_\infty. \quad (11)$$

$$\|X_+ - Y_+\|_\infty \leq \left(\frac{1}{2} + \frac{2}{\pi} + \frac{1}{\pi} \log \left(\frac{\|X\|_\infty + \|Y\|_\infty}{\|X - Y\|_\infty} \right) \right) \|X - Y\|_\infty. \quad (12)$$

Proof. We begin with an observation that given a symmetric matrix, $X \in \mathbb{S}_n$, we can construct the PSD projection using the polar decomposition of X as follows,

$$X_+ = \frac{X + (X^\top X)^{\frac{1}{2}}}{2}. \quad (13)$$

Note, $(X^\top X)^{\frac{1}{2}} \neq X$ unless $X \in \mathbb{S}_n^+$ (this follows from the definition of a square root). Eq. (13) follows by considering eigen-decomposition of $X = UDU^\top$ and then noting that $\frac{X + (X^\top X)^{\frac{1}{2}}}{2} = U \text{diag} \left(\frac{D_{1,1} + |D_{1,1}|}{2}, \dots, \frac{D_{n,n} + |D_{n,n}|}{2} \right) U^\top = UD_+U^\top$, using the fact that $\max\{x, 0\} = \frac{x + |x|}{2}$.

Now it follows from Eq. (13) and the triangle inequality that,

$$\begin{aligned}\|X_+ - Y_+\| &= \frac{1}{2}\|X - Y + (X^\top X)^{\frac{1}{2}} - (Y^\top Y)^{\frac{1}{2}}\| \\ &\leq \frac{1}{2}\left(\|X - Y\| + \|(X^\top X)^{\frac{1}{2}} - (Y^\top Y)^{\frac{1}{2}}\|\right),\end{aligned}\quad (14)$$

where $\|\cdot\|$ is any valid matrix norm.

To deduce Eq. (10) we simply apply Lemma 5, $\|(A^\top A)^{\frac{1}{2}} - (B^\top B)^{\frac{1}{2}}\|_2 \leq \|A - B\|_2$, to Eq. (14) when the matrix norm is the Frobenious norm.

To deduce Eq. (11) we use the equivalence between the spectral norm and Frobenius norm: $\|A\|_\infty \leq \|A\|_2 \leq \sqrt{n}\|A\|_\infty$ for any $A \in \mathbb{S}_n$. Then by Lemma 5 and Eq. (14) we have that,

$$\begin{aligned}\|X_+ - Y_+\|_\infty &\leq \frac{1}{2}\left(\|X - Y\|_\infty + \|(X^\top X)^{\frac{1}{2}} - (Y^\top Y)^{\frac{1}{2}}\|_\infty\right) \\ &\leq \frac{1}{2}\|X - Y\|_\infty + \frac{1}{2}\|(X^\top X)^{\frac{1}{2}} - (Y^\top Y)^{\frac{1}{2}}\|_2 \\ &\leq \frac{1}{2}\|X - Y\|_\infty + \frac{1}{2}\|X - Y\|_2 \leq \frac{1}{2}(1 + \sqrt{n})\|X - Y\|_\infty.\end{aligned}$$

Eq. (12) follows by applying Lemma 6 to Eq. (14). \square

Further to Proposition 1, if we assume X and Y are non-singular then we may improve the spectral norm bounds of Eqs (11) and (12) by following the same argument of applying Eq. (14) and using the inequalities for $\|(X^\top X)^{\frac{1}{2}} - (Y^\top Y)^{\frac{1}{2}}\|_\infty$ from [30]. Moreover, using the same proof strategy we may derive a bound for $\|X_+ - Y_+\|$ with respect to the Schatten 1-norm from the Powers–Størmer inequality (Lem. 4.1 in [31]).

Using the bounds from Proposition 1 we next bound the expected error of using Algorithm 2 in both norms. These error bounds will involve the following terms, defined for some $X \in \mathbb{S}_n$ and $k, l, q \in \mathbb{N}$,

$$\varepsilon_1(\{\sigma_i\}_{i=1}^n, k, l) := \sqrt{\left(1 + \frac{k}{l-1}\right)\left(\sum_{j>k} \sigma_j^2\right)}.\quad (15)$$

$$\varepsilon_2(\sigma, k, l, q) := \left(1 + \sqrt{\frac{k}{l-1}} + \frac{e\sqrt{k+l}}{l}\sqrt{n-k}\right)^{\frac{1}{2q+1}}\sigma.\quad (16)$$

Corollary 1. Consider $X \in \mathbb{S}_n$. Choose a target rank $k \geq 2$ and an oversampling parameter $l \geq 2$, where $k + l \leq n$. Execute Algorithm 2 with $q = 0$ to get an output of $\hat{X}_+ \in \mathbb{S}_n$, then

$$\mathbb{E}[\|X_+ - \hat{X}_+\|_2] \leq (1 + \sqrt{k+l})\varepsilon_1(\{\sigma_i(X)\}_{i=1}^n, k, l). \quad (17)$$

Execute Algorithm 2 for some $q \in \mathbb{N}$ to get an output of $\hat{X}_+ \in \mathbb{S}_n$, then

$$\begin{aligned} \mathbb{E}[\|X_+ - \hat{X}_+\|_\infty] \leq \min \Bigg\{ & (1 + \sqrt{n})\varepsilon_2(\sigma_{k+1}(X), k, l, q), \\ & \left(1 + \frac{4}{\pi} + \frac{2}{\pi}(\log(2\sigma_1(X)))\right) \varepsilon_2(\sigma_{k+1}(X), k, l, q) \\ & + \frac{1}{\pi} \min\{e^{-1}, \sqrt{2\varepsilon_2(\sigma_{k+1}(X), k, l, q)}\} \Bigg\}, \end{aligned} \quad (18)$$

where the expectations of Eqs (17) and (18) is taken with respect to the randomly generated matrix Ω and the ε_i terms can be found in Eqs (15) and (16).

Proof. Since $Q \in \mathbb{R}^{n \times (k+l)}$ we have that $\text{rank } Q \leq k + l$. By a similar argument used to show Eq. (9) it then follows $\|QQ^\top\|_2 \leq \sqrt{k+l}$.

From Eqs (6) and (10) we obtain

$$\begin{aligned} \|X_+ - \hat{X}_+\|_2 &\leq \|X - \hat{X}\|_2 = \|X - QQ^\top X QQ^\top\|_2 \\ &\leq (1 + \sqrt{k+l})\|X - QQ^\top X\|_2. \end{aligned}$$

Eq. (17) then follows by applying Thm. 2 in the appendix. We now show Eq. (18). From Eqs (4) and (11) we have

$$\begin{aligned} \|X_+ - \hat{X}_+\|_\infty &\leq \frac{1}{2}(\sqrt{n} + 1) \|X - QQ^\top X QQ^\top\|_\infty \\ &\leq (\sqrt{n} + 1) \|X - QQ^\top X\|_\infty. \end{aligned} \quad (19)$$

Moreover, from Eq. (12) we have that

$$\begin{aligned} \|X_+ - \hat{X}_+\|_\infty &\leq \left(\frac{1}{2} + \frac{2}{\pi} + \frac{1}{\pi} \log \left(\frac{\|X\|_\infty + \|\hat{X}\|_\infty}{\|X - \hat{X}\|_\infty} \right) \right) \|X - \hat{X}\|_\infty \\ &= \left(\frac{1}{2} + \frac{2}{\pi} + \frac{1}{\pi} \log \left(\|X\|_\infty + \|\hat{X}\|_\infty \right) \right) \|X - \hat{X}\|_\infty \\ &\quad - \frac{1}{\pi} \log(\|X - \hat{X}\|_\infty) \|X - \hat{X}\|_\infty. \end{aligned} \quad (20)$$

We now bound various terms in Eq. (20). Firstly, by the sub-multiplicative property of Schatten norms we have that $\|\hat{X}\|_\infty = \|QQ^\top X QQ^\top\|_\infty \leq \|QQ^\top\|_\infty^2 \|X\|_\infty = \|X\|_\infty$ and hence by the monotonicity property of the logarithm and Eq. (8) it follows that,

$$\log(\|X\|_\infty + \|\hat{X}\|_\infty) \leq \log(2\sigma_1(X)). \quad (21)$$

Now, applying the log inequality in Eq. (48) (found in the Appendix), Eq. (4) and the monotonicity property of the square root, it follows that

$$\begin{aligned} -\log(\|X - \hat{X}\|_\infty) \|X - \hat{X}\|_\infty &\leq \min \left\{ e^{-1}, \sqrt{\|X - \hat{X}\|_\infty} \right\} \\ &\leq \min \left\{ e^{-1}, \sqrt{2\|X - QQ^\top X\|_\infty} \right\}. \end{aligned} \quad (22)$$

Applying the bounds in Eqs (4), (21) and (22) along with Jensen's inequality, and noting $f(x) = \min\{e^{-1}, \sqrt{2x}\}$ is a concave function, to Eq. (20) we get that

$$\begin{aligned} \mathbb{E}[\|X_+ - \hat{X}_+\|_\infty] &\leq \left(1 + \frac{4}{\pi} + \frac{2}{\pi} \log(2\sigma_1(X))\right) \mathbb{E}[\|X - QQ^\top X\|_\infty] \\ &\quad + \frac{1}{\pi} \mathbb{E}[\min \left\{ e^{-1}, \sqrt{2\|X - QQ^\top X\|_\infty} \right\}] \\ &\leq \left(1 + \frac{4}{\pi} + \frac{2}{\pi} \log(2\sigma_1(X))\right) \mathbb{E}[\|X - QQ^\top X\|_\infty] \\ &\quad + \frac{1}{\pi} \min \left\{ e^{-1}, \sqrt{2\mathbb{E}[\|X - QQ^\top X\|_\infty]} \right\}. \end{aligned} \quad (23)$$

Applying the monotonicity of the square root function and Eq. (45) (from Thm. 2 in the appendix) to both Eqs (19) and (23) and taking the minimum of these inequalities we deduce Eq. (18). \square

3.0.2 A Scaled Randomized PSD Projection

Symmetric matrices have the special property that the absolute values of their eigenvalues are exactly equal to their singular values, i.e., $\{|\lambda_1(X)|, \dots, |\lambda_n(X)|\} = \{\sigma_1(X), \dots, \sigma_n(X)\}$. As a result, the PSD projection of the optimal rank- k approximation of a symmetric matrix is not necessarily equal to the rank- k matrix whose PSD projection best approximates the projection of the entire original matrix. To see this consider the following example.

Algorithm 3 Scaled Randomized PSD Projection

Function $\hat{X}_+ = \text{ran_proj_scal}(X, k, l, q, \alpha)$.

Input: $X \in \mathbb{S}_n, k \in \mathbb{N}, l \in \mathbb{N}, \alpha > 0$.

Output: $\hat{X}_+ \in \mathbb{S}_n^+$.

- 1: $B = (X + \alpha I)/\alpha$
 - 2: $Q = \text{range_finder}(B, k, l, q)$ \triangleright Algorithm 1
 - 3: $[U, D] = \text{eig}(Q^\top B Q)$ $\triangleright Q^\top B Q = U D U^\top$
 - 4: $\hat{X}_+ = \alpha Q U (\max(D, 1) - I) U^\top Q^\top$
-

Counterexample 1. Let $X = \text{diag}([-3, -2, 1])$. Clearly the optimal rank-1 approximation of X is $\hat{X} = \text{diag}([-3, 0, 0])$ since the -3 element corresponds to the maximal singular value. However $\hat{X}_+ = 0_{3 \times 3}$. Alternatively the rank-1 matrix $\tilde{X} = \text{diag}([0, 0, 1])$ is a worse approximation of X but has the same PSD projection as X : $\tilde{X}_+ = X_+$.

Unfortunately, Algorithm 2 works by approximating a given matrix $X \in \mathbb{S}_n$ by a lower rank matrix $X \approx \hat{X} = Q Q^\top X Q Q^\top$ and then projecting \hat{X} . Clearly, our projection method might suffer from large errors when projecting matrices whose largest singular values correspond to negative eigenvalues, as demonstrated by Counterexample 1. To overcome this issue we next show how scaling can be used to ensure that the maximum positive eigenvalues correspond to the maximum singular values.

Lemma 2. Consider $X \in \mathbb{S}_n$. Suppose $\alpha := |\min_i \lambda_i(X)| > 0$. Then $B := \frac{X + \alpha I}{\alpha}$ is a PSD symmetric matrix whose singular values and eigenvalues are such that

$$\sigma_i(B) = \lambda_i(B) = \frac{\lambda_i(X) + \alpha}{\alpha}. \quad (24)$$

Moreover, $\lambda_i(X) < 0$ iff $\sigma_i(B) \in [0, 1)$ and $\lambda_i(X) \geq 0$ iff $\sigma_i(B) \in [1, \infty)$.

Proof. $X \in \mathbb{S}_n$ is a symmetric matrix and hence diagonalizable. Let $X = U D U^\top$ be the eigen-decomposition of X . It follows that $B := (X + \alpha I)/\alpha$ is simultaneously diagonalizable with $B = U (D/\alpha + I) U^\top$. Therefore the eigenvalues of B are equal to $\frac{\lambda_i(X) + \alpha}{\alpha}$. Moreover, since $\alpha := |\min_i \lambda_i(X)|$ it follows that all of the eigenvalues are positive and therefore $B \in \mathbb{S}_n^+$. The singular values and eigenvalues of PSD matrices are equivalent, thus proving Eq. (24). Finally, if $\lambda_i(X) < 0$ then $\sigma_i(B) < \alpha/\alpha = 1$. \square

If we approximate $B := \frac{X + \alpha I}{\alpha}$ by $\hat{B} \approx QQ^\top BQQ^\top$, we capture information about the leading singular values of B , which correspond to the dominant positive eigenvalues of X (by Lemma 2). This enables us to retain the most important information for an approximate PSD projection. Moreover, this scaling is particularly well suited to the power iteration method. As shown in Lemma 2, the negative eigenvalues of X correspond to the singular values of B in the interval $[0, 1]$, which are progressively compressed to zero as q increases in Algorithm 1. After approximating B by \hat{B} , we can then project and re-scale \hat{B} to derive an approximation of X_+ . This method is summarized in Algorithm 3. We now derive error bounds for computing an approximate PSD projection using Algorithm 3. To do this, we first prove a key preliminary result that expresses the approximate PSD projection from Algorithm 3 in terms of B .

Lemma 3. *Consider $X \in \mathbb{S}_n$, $k \geq 2$, $k + l \leq n$, $q \in \mathbb{N}$ and $\alpha := |\min_i \lambda_i(X)| > 0$. Execute the scaled randomized PSD algorithm (Algorithm 3) to get an output of $\hat{X}_+ \in \mathbb{S}_n$ then*

$$\hat{X}_+ = \alpha(QQ^\top(B - I)QQ^\top)_+, \quad (25)$$

where matrices B and Q are found in Lines 1 and 2 respectively in Algorithm 3.

Proof. From Algorithm 3 we have $\hat{X}_+ = \alpha Q \hat{U}(\max(\hat{D}, 1) - I) \hat{U}^\top Q^\top$ where $\hat{U} \hat{D} \hat{U}^\top = Q^\top B Q$ and $\hat{U} \hat{U}^\top = \hat{U}^\top \hat{U} = I$. Therefore, using $Q^\top Q = I$ and Lemma 8 (found in the Appendix) we have that

$$\begin{aligned} \hat{X}_+ &= \alpha Q \hat{U}(\max(\hat{D}, 1) - I) \hat{U}^\top Q^\top = \alpha Q \hat{U}(D - I)_+ \hat{U}^\top Q^\top \\ &\stackrel{(49)}{=} \alpha Q(\hat{U}(D - I) \hat{U}^\top)_+ Q^\top = \alpha Q(Q^\top B Q - I)_+ Q^\top \\ &= \alpha Q(Q^\top B Q - Q^\top Q)_+ Q^\top = \alpha Q(Q^\top(B - I)Q)_+ Q^\top \\ &\stackrel{(49)}{=} \alpha(QQ^\top(B - I)QQ^\top)_+. \end{aligned}$$

□

We now use Lemma 3 to derive error bounds for the quality of the PSD projection given by Algorithm 3 in both the Frobenius and spectral norms.

Proposition 2. *Consider $X \in \mathbb{S}_n$ and $\alpha := |\min_i \lambda_i(X)| > 0$. Choose a target rank $k \geq 2$ and an oversampling parameter $l \geq 2$, where $k + l \leq n$. Execute the scaled randomized PSD algorithm (Algorithm 3) with $q = 0$ to get an output of $\hat{X}_+ \in \mathbb{S}_n$. Then*

$$\mathbb{E}[\|X_+ - \hat{X}_+\|_2] \leq \alpha \sqrt{n - k} + (1 + \sqrt{k + l}) \varepsilon_1(\{(\lambda_i(X) + \alpha)\}_{i=1}^n, k, l). \quad (26)$$

Execute the scaled randomized PSD algorithm (Algorithm 3) for some $q \in \mathbb{N}$ to get an output of $\hat{X}_+ \in \mathbb{S}_n$, then

$$\begin{aligned} \mathbb{E}[\|X_+ - \hat{X}_+\|_\infty] \leq \min & \left\{ (1 + \sqrt{n})(\varepsilon_2((\lambda_{k+1}(X) + \alpha), k, l, q) + \alpha/2), \right. \\ & \left(\frac{1}{2} + \frac{2}{\pi} + \frac{1}{\pi}(\log(2\sigma_1(X))) \right) (2\varepsilon_2((\lambda_{k+1}(X) + \alpha), k, l, q) + \alpha) \\ & \left. + \frac{1}{\pi} \min\{e^{-1}, \sqrt{2\varepsilon_2((\lambda_{k+1}(X) + \alpha), k, l, q) + \alpha}\} \right\} \end{aligned} \quad (27)$$

where the expectation is taken with respect to the randomly generated matrix Ω and the ε_i terms can be found in Eqs (15) and (16).

Proof. Let $B := (X + \alpha I)/\alpha$. Then since $\alpha > 0$ and hence it follows that

$$X_+ = \alpha(B - I)_+. \quad (28)$$

We split the proof into two parts. In part one we show our Frobenius norm error bound, given in Eq. (26). In part two we show our spectral norm error bound given in Eq. (27).

Part One: Since $Q \in \mathbb{R}^{n \times (k+l)}$ we have that $\text{rank } Q \leq k + l$. By a similar argument used to show Eq. (9) it then follows $\|QQ^\top\|_2 \leq \sqrt{k+l}$. It now follows using $\|QQ^\top\|_2 \leq \sqrt{k+l}$ and the triangle inequality that,

$$\begin{aligned} \|X_+ - \hat{X}_+\|_2 & \stackrel{(28)}{=} \|\alpha(B - I)_+ - \hat{X}_+\|_2 \\ & \stackrel{(25)}{=} \|\alpha(B - I)_+ - \alpha(QQ^\top(B - I)QQ^\top)_+\|_2 \\ & \leq \alpha\|(B - I)_+ - (QQ^\top(B - I)QQ^\top)_+\|_2 \\ & \stackrel{(10)}{\leq} \alpha\|(B - I) - (QQ^\top(B - I)QQ^\top)\|_2 \\ & = \alpha\|(B - (QQ^\top BQQ^\top)) + (QQ^\top - I)\|_2 \\ & \leq \alpha\|(B - (QQ^\top BQQ^\top))\|_2 + \alpha\|QQ^\top - I\|_2 \\ & \stackrel{(6)}{\leq} \alpha(1 + \sqrt{k+l})\|B - QQ^\top B\|_2 + \alpha\|I - QQ^\top\|_2. \end{aligned} \quad (29)$$

We now take the expectation. Note that $Q = \text{range_finder}[X, k, l, q]$ satisfies $\text{rank}(Q) \geq k$ with probability one, as $X\Omega$ will almost certainly have a row rank greater than k (as shown on Page 57 in the proof of Theorem 10.5 in [13]). Therefore, by a similar argument to Eq. (7) it follows

$$E[\|I - QQ^\top\|_2] \leq \sqrt{n - k}. \quad (30)$$

We next bound $\alpha \mathbb{E}[\|(I - QQ^\top)B\|_2]$ in Eq. (29).

$$\begin{aligned}
\alpha \mathbb{E}[\|(I - QQ^\top)B\|_2] &\stackrel{(46)}{\leq} \alpha \sqrt{\left(1 + \frac{k}{l-1}\right) \left(\sum_{j>k} \sigma_j(B)^2\right)} \\
&\stackrel{(24)}{=} \alpha \sqrt{\left(1 + \frac{k}{l-1}\right) \left(\sum_{j>k} \left(\frac{\lambda_j(X) + \alpha}{\alpha}\right)^2\right)} \stackrel{(15)}{=} \varepsilon_1(\{(\lambda_i(X) + \alpha)\}_{i=1}^n, k, l).
\end{aligned} \tag{31}$$

Combining bounds from Eqs (29), (30) and (31) we get Eq. (26).

Part Two: We now show Eq. (27). First note by Eq. (7) that the eigenvalues of QQ^\top are either zero or one, implying $\|I - QQ^\top\|_\infty \leq 1$. Now, using the triangle inequality along with Eqs (4) and (11) we get that,

$$\begin{aligned}
\mathbb{E}[\|X_+ - \hat{X}_+\|_\infty] &\leq \alpha \mathbb{E}[\|(B - I)_+ - (QQ^\top(B - I)QQ^\top)_+\|_\infty] \\
&\stackrel{(11)}{\leq} \frac{\alpha}{2}(1 + \sqrt{n}) \mathbb{E}[\|(B - I) - (QQ^\top(B - I)QQ^\top)\|_\infty] \\
&\leq \frac{\alpha}{2}(1 + \sqrt{n}) \mathbb{E}[\|(B - (QQ^\top BQQ^\top))\|_\infty + \|QQ^\top - I\|_\infty] \\
&\stackrel{(4)}{\leq} \alpha(1 + \sqrt{n}) \mathbb{E}[\|B - QQ^\top B\|_\infty] + \frac{\alpha}{2}(1 + \sqrt{n}).
\end{aligned} \tag{32}$$

By Eq. (25) we have that $\hat{X}_+ = \alpha(QQ^\top(B - I)QQ^\top)_+$ and hence $\hat{X} = \alpha(QQ^\top(B - I)QQ^\top) = QQ^\top XQQ^\top$. Now, by a similar argument to Eq. (23) we get,

$$\begin{aligned}
\mathbb{E}[\|X_+ - \hat{X}_+\|_\infty] &\leq \mathbb{E}\left[\alpha \left(\frac{1}{2} + \frac{2}{\pi} + \frac{1}{\pi} \log(\|X\|_\infty + \|QQ^\top XQQ^\top\|_\infty)\right) \right. \\
&\quad \left. \times \|B - I - QQ^\top(B - I)QQ^\top\|_\infty - \frac{1}{\pi} \log(\|X - \hat{X}\|_\infty) \|X - \hat{X}\|_\infty \right] \\
&\leq \mathbb{E}\left[\alpha \left(\frac{1}{2} + \frac{2}{\pi} + \frac{1}{\pi} \log(2\sigma_1(X))\right) (\|I - QQ^\top BQQ^\top\|_\infty + \|I - QQ^\top\|_\infty) \right. \\
&\quad \left. + \frac{1}{\pi} \min \left\{e^{-1}, \sqrt{\alpha\|I - QQ^\top BQQ^\top\|_\infty + \alpha\|I - QQ^\top\|_\infty}\right\} \right] \\
&\leq \left(\frac{1}{2} + \frac{2}{\pi} + \frac{1}{\pi} \log(2\sigma_1(X))\right) (2\alpha \mathbb{E}[\|B - QQ^\top B\|_\infty] + \alpha) \\
&\quad + \frac{1}{\pi} \min \left\{e^{-1}, \sqrt{2\alpha \mathbb{E}[\|I - QQ^\top B\|_\infty] + \alpha}\right\}.
\end{aligned} \tag{33}$$

We next bound $\alpha \mathbb{E}[\|(I - QQ^\top)B\|_\infty]$ in Eqs (32) and (33):

$$\begin{aligned}
& \alpha \mathbb{E}[\|(I - QQ^\top)B\|_\infty] \tag{34} \\
& \stackrel{(45)}{\leq} \left(1 + \sqrt{\frac{k}{l-1}} + \frac{e\sqrt{k+l}}{l} \sqrt{\min\{m, n\} - k}\right)^{\frac{1}{2q+1}} \alpha \sigma_{k+1}(B) \\
& \stackrel{(24)}{=} \left(1 + \sqrt{\frac{k}{l-1}} + \frac{e\sqrt{k+l}}{l} \sqrt{\min\{m, n\} - k}\right)^{\frac{1}{2q+1}} (\lambda_{k+1}(X) + \alpha) \\
& \stackrel{(16)}{=} \varepsilon_2((\lambda_{k+1}(X) + \alpha), k, l, q).
\end{aligned}$$

Where inequality (45) is from [13] and provided in the appendix. Applying this to the bounds given in Eqs (32) and (33) and taking the minimum of these bounds we derive Eq. (27). \square

Although the error bounds given in Eqs (26) and (27) are not tight they are informative to when the scaled randomized PSD projection (Algorithm 3) outperforms the randomized PSD projection without scaling (Algorithm 2). Suppose X has $r \in \mathbb{N}$ negative eigenvalues and these negative eigenvalues are clustered near the minimal eigenvalue, that is $|\lambda_i(X)| \approx \alpha = |\min_i \lambda_i(X)|$ for $i \in \{n-r, \dots, n\}$. Then if the rank of the projection is selected to be greater than or equal to the number of positive eigenvalues, $k \geq n - r$, it follows that the sum $\sum_{i>k}^n (\lambda_i(X) + \alpha)^2$, involved in the Frobenius error bound given in Eq. (26), or term $(\lambda_{k+1}(X) + \alpha)$, involved in the spectral error bound given in Eq. (27), are small. In the following corollary we give an example of a class matrices $X \in \mathbb{S}_n$ such that the right hand side of the bound given in Eq. (17) is greater than right hand side of the bound given in Eq. (26). This indicates that, for at least this class of, it is more accurate to use the scaled randomized PSD projection (Algorithm 3) than the randomized PSD projection without scaling (Algorithm 2). Note that we can also construct a similar example for the spectral radius but omit this for the sake of brevity. In Figure 3 we plot the eigen and singular values for a particular instance of a matrix within this class for $n = 1000$.

Corollary 2. *Consider the following matrix,*

$$X = Y^\top \text{diag}([-\beta_1 \mathbf{1}_{n/4}, -\beta_2 \mathbf{1}_{4/2}, \beta_3 \mathbf{1}_{n/4}, \beta_4 \mathbf{1}_{4/2}])Y \in \mathbb{S}_n, \tag{35}$$

where $Y \in \mathbb{S}_n$ is an orthogonal matrix and $\beta_3 > \beta_1 > \beta_4 > \beta_2 > 0$. Then if $\alpha := |\min_i \lambda_i(X)|$, $k = n/2$, $l \in \mathbb{N}$ and $n \geq 2(l-1) \left(\frac{2\beta_1^2}{(\sqrt{\beta_4^2 + \beta_2^2} - |\beta_1 - \beta_2|)^2} - 1 \right)$

we have that $E_2 \leq E_1$, where

$$\begin{aligned} E_1 &:= (1 + \sqrt{k + l}) \varepsilon_1(\{\sigma_i(X)\}_{i=1}^n, k, l), \\ E_2 &:= \alpha \sqrt{n - k} + (1 + \sqrt{k + l}) \varepsilon_1(\{(\lambda_i(X) + \alpha)\}_{i=1}^n, k, l), \end{aligned}$$

with the ε_i terms from Eqs (15) and (16).

Proof. It follows that

$$\sigma_i(X) = \begin{cases} \beta_3 & 1 \leq i \leq n/4 \\ \beta_1 & n/4 < i \leq n/2 \\ \beta_4 & n/2 < i \leq 3n/4 \\ \beta_2 & 3n/4 < i \leq n \end{cases} \quad \lambda_i(X) = \begin{cases} \beta_3 & 1 \leq i \leq n/4 \\ \beta_4 & n/4 < i \leq n/2 \\ -\beta_2 & n/2 < i \leq 3n/4 \\ -\beta_1 & 3n/4 < i \leq n \end{cases}$$

Hence $\alpha = \beta_1$ (the magnitude of the most negative eigenvalue). Now, $E_1 = (1 + \sqrt{k + l}) \sqrt{1 + \frac{k}{l-1}} \sqrt{\sum_{j>k} \sigma_j^2} = (1 + \sqrt{n/2 + l}) \sqrt{1 + \frac{n}{2(l-1)}} \sqrt{\frac{n}{4}(\beta_3^2 + \beta_2^2)}$.

Moreover, $E_2 = \beta_1 \sqrt{n/2} + (1 + \sqrt{n/2 + l}) \sqrt{1 + \frac{n}{2(l-1)}} \sqrt{\frac{n}{4}(\beta_1 - \beta_2)^2}$.

Since $n \geq 2(l-1) \left(\frac{2\beta_1^2}{(\sqrt{\beta_4^2 + \beta_2^2} - |\beta_1 - \beta_2|)^2} - 1 \right)$ it follows that $\frac{\sqrt{2}\beta_1}{\sqrt{\beta_4^2 + \beta_2^2} - |\beta_1 - \beta_2|} \leq \sqrt{1 + \frac{n}{2(l-1)}} \leq (1 + \sqrt{n/2 + l}) \sqrt{1 + \frac{n}{2(l-1)}}$. Rearranging this we get

$$\beta_1 \sqrt{n/2} \leq \sqrt{n/4} (1 + \sqrt{n/2 + l}) \sqrt{1 + \frac{n}{2(l-1)}} (\sqrt{\beta_4^2 + \beta_2^2} - (\sqrt{\beta_1 - \beta_2})^2).$$

It follows from this inequality that $E_2 \leq E_1$. \square

To execute Algorithm 3 we estimate $\alpha \approx |\min_i \lambda_i(X)|$. Fortunately, such an estimation can be cheaply computed using the classical power iteration method that dates back to the 1920's [32, 33], see Algorithm 4 for the basic procedure. The maximum singular value of a symmetric matrix, estimated using Algorithm 4, either corresponds to the absolute value of the minimal or maximal eigenvalue. We are only interested in computing the absolute value of the minimal eigenvalue. Therefore, to find the minimal eigenvalue we must then make the following transformation: $Y = X - \sigma_1(X)I$. It follows that $|\min_i \lambda_i(X)| = |\sigma_1(Y) - \sigma_1(X)|$, as shown in Lemma 9. The entire procedure for calculating the absolute value of the minimal eigenvalue is summarized in Algorithm 5.

Algorithm 4 Approximate maximum singular value

Function $\sigma_1 = \text{power_iteration}(X, N)$.

Input: $X \in \mathbb{S}_n, N \in \mathbb{N}$.

Output: $\sigma_1 > 0$.

- 1: $v = \text{randn}(n, 1)$ ▷ Random initialization with $v_i \stackrel{(iid)}{\sim} \mathcal{N}(0, 1)$
 - 2: **for** $i = 1 : N$ **do**
 - 3: $v = Xv / \|Xv\|_2$
 - 4: **end for**
 - 5: $\sigma_1 = \|Xv\|_2$
-

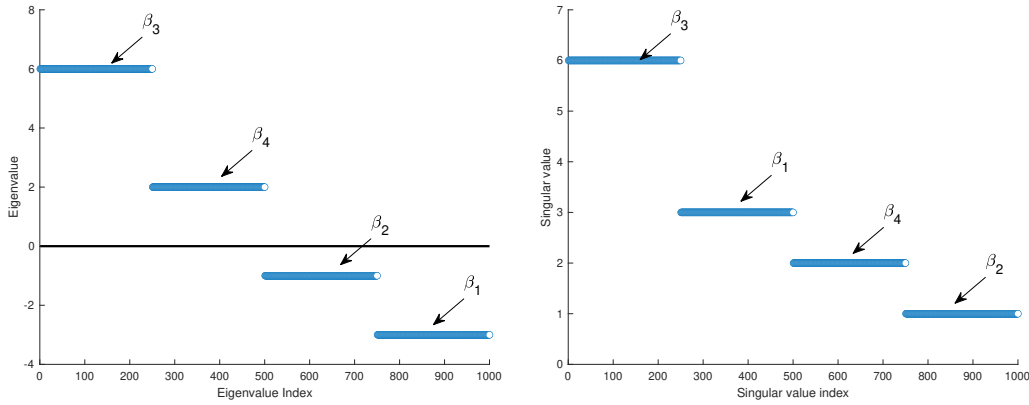
Algorithm 5 Approximate absolute value of minimum eigenvalue

Function $\lambda_{\min} = \text{min_eig}(X, N)$.

Input: $X \in \mathbb{S}_n, N \in \mathbb{N}$.

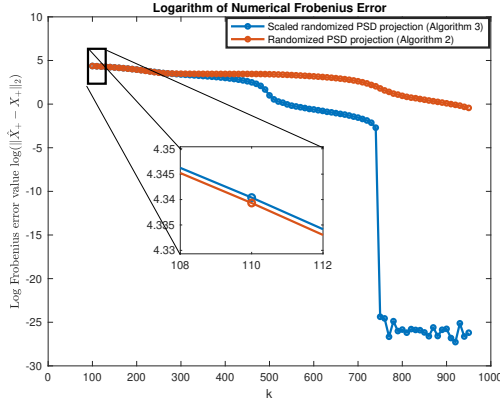
Output: $\lambda_{\min} > 0$.

- 1: $\sigma_1 = \text{power_iteration}(X, N)$ ▷ Algorithm 4
 - 2: $Y = X - \sigma_1 I$
 - 3: $\sigma_2 = \text{power_iteration}(Y, N)$ ▷ Algorithm 4
 - 4: $\lambda_{\min} = |\sigma_1 - \sigma_2|$
-

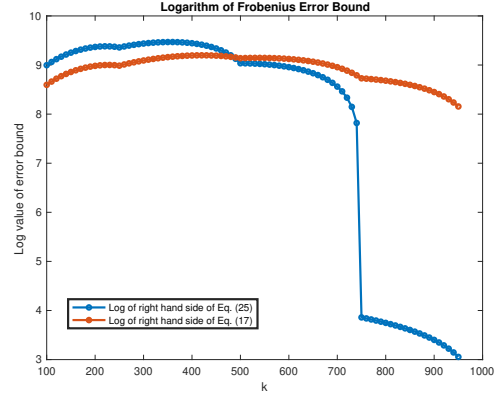


(a) Eigenvalues $\lambda_1(X) > \lambda_2(X) > 0 > \lambda_3(X) > \lambda_4(X)$. (b) Singular values $\sigma_1(X) > \sigma_2(X) > \sigma_3(X) > \sigma_4(X) > 0$.

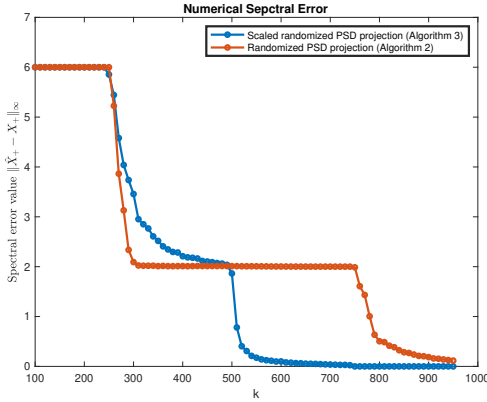
Figure 3: Plot showing the distribution of eigenvalues and singular values of the matrix given in Eq. (35) and corresponding associated scalars $\beta_3 > \beta_1 > \beta_4 > \beta_2 > 0$.



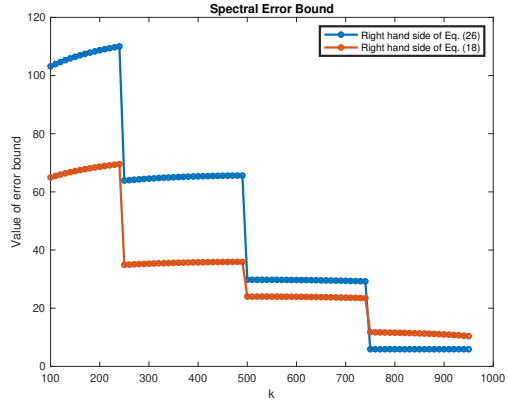
(a) Logarithm of numerical Frobenius error of Algs 2 and 3.



(b) Logarithm of Frobenius error bounds of Eqs (17) and (26).



(c) Numerical spectral error of Algorithms 2 and 3.



(d) Spectral error bounds of Eqs (18) and (27).

Figure 4: Accuracy of projecting X from Eq. (35) with $n = 1000$, $\beta_1 = 3$, $\beta_2 = 1$, $\beta_3 = 6$, $\beta_4 = 2$ and Y randomly generated using Algorithms 2 and 3 under $l = 5$, $q = 2$ and varying $k \in \mathbb{N}$. The true PSD projections are calculated using Eq. (2), where the eigen-decomposition is calculated using Matlab's `eig` function.

3.0.3 PSD Projection Numerical Examples

We next numerically analyze the performance of Algorithms 2 and 3, where the magnitude of the smallest eigenvalue, α , is computed using Algorithm 5. We first consider the case of projecting $X \in \mathbb{S}_n$ from Eq. (35) when $\beta_1 = 3, \beta_2 = 1, \beta_3 = 6, \beta_4 = 2$ and $n = 1000$. Figure 3 shows the eigen and singular value distribution of X . We note that we have chosen this test case because the spectral profile of X is representative of the most “unfriendly” matrix class we are likely to encounter. Sub-figures 4b and 4d show how the error bounds in the Frobenius and spectral norms change with k , the number of random samples used in the Randomized Range Finder (Algorithm 1). These apriori error bounds are based only on the singular values and eigenvalues of $X \in \mathbb{S}_n$ and can be calculated without computing the full matrix projection. In both norms, we see that the red curve is initially lower than the blue curve showing that the error bound of projecting with Algorithm 2 is smaller than that of using Algorithm 3. This is because the first $n/4$ positive eigenvalues are equal to the leading order singular values, corresponding to β_3 . However, the next $n/4$ singular values correspond to β_1 that is associated with a negative eigenvalue. For this reason it is better to use the Scaled Randomized PSD Projection (Algorithm 3) when $k > n/4$. We see this intuition reflected in Figure 4 where for sufficiently large k the blue curve becomes less than the red curve. This occurs in both the numerically calculated projection errors and the theoretical projection error bounds, although this is only seen for large k in the theoretical projection bounds.

Note that $X \in \mathbb{S}_n$ from Eq. (35) has no zero eigenvalues, indicating that it is full rank. Consequently, it is expected that our proposed approximated PSD projection will exhibit reduced performance, as it involves first approximating the matrix by a low-rank matrix. We next project several matrices obtained from practical applications. In each case n exceeds 10,000. As shown by the eigenvalues plotted in Fig. 5, many of these matrices are low rank or approximately low rank, with many eigenvalues close to zero. The numerical performance of our projection methods with Frobenius errors is given in Table 1. For brevity we only consider the Frobenius norm and will not consider the spectral norm. The optimal PSD projection, X_+ , is computed using Matlab’s `eig` routine and Eq. (2), whereas the RNLA projection, \hat{X}_+ , is computed by executing either Alg. 2 or Alg. 3. Each numerical experiment was conducted with $l = 10$ and $q = 4$. For scaled projections the scaling factor was set to $\alpha = |\min_i \lambda_i(X)|$ where α was estimated using Alg. 5 with $N = 10$.

As expected, the projection error decreases as k increases (although we main-

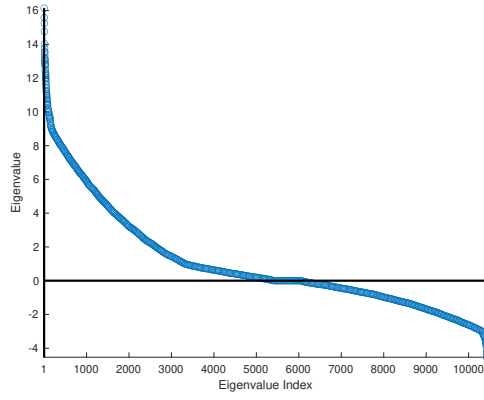
skirt.mat n=12,598	k=[0.01n] Scaled: Alg. 3	k=[0.25n] Scaled: Alg. 3	k=[0.5n] Scaled: Alg. 3	k=[0.01n] Alg. 2	k=[0.25n] Alg. 2	k=[0.5n] Alg. 2
$\ X - QQ^T X\ _2$	390.2	142.7	109.2	389.73	106.6	45.2
$\ X_+ - \tilde{X}_+\ _2$	360.2	39.4	5.43	360	73	32
shuttle_eddy.mat n=10,429						
$\ X - QQ^T X\ _2$	298.22	114.19	80.89	297.94	108.99	43.09
$\ X_+ - \tilde{X}_+\ _2$	279.7	49.1	7.7	279.38	69.69	29.89
cyl6.mat n=13,681						
$\ X - QQ^T X\ _2$	3.82e+3	1.07e+3	0.97e+3	3.8e+3	210.96	216.05
$\ X_+ - \tilde{X}_+\ _2$	3.44e+3	52.62	27.86	3.43e+3	149.4	151.7
lowThrust_13.mat n=18,476						
$\ X - QQ^T X\ _2$	896.15	697.85	655.7	877.48	334.17	292.26
$\ X_+ - \tilde{X}_+\ _2$	612.85	287.16	169.38	635.46	242.26	209.39
G57.mat n=5,000						
$\ X - QQ^T X\ _2$	139.28	107.1	93.1	139.14	94.78	52.29
$\ X_+ - \tilde{X}_+\ _2$	96.96	38.46	3.41	99.51	70.84	39.2
G67.mat n=10,000						
$\ X - QQ^T X\ _2$	197.21	151.5	132.32	197.03	134.24	74.09
$\ X_+ - \tilde{X}_+\ _2$	137.48	54.61	4.69	140.77	100.34	55.56

Table 1: Errors associated with finding RNLA and deterministic PSD projections of benchmark matrices from [34].

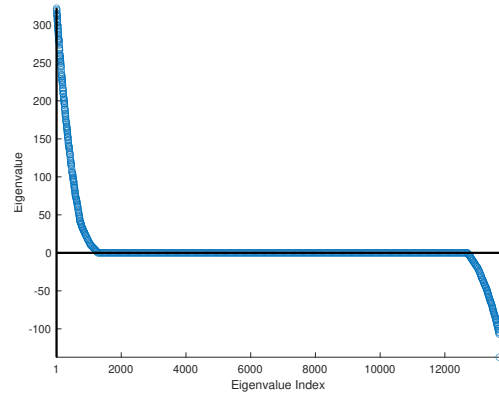
tain $k \ll n$). The scaled randomized projection, Alg. 3, mostly outperforms the vanilla randomized projection, Alg. 2, even though the error $\|X - QQ^T X\|_2$ is often larger for the scaled projection. The `shuttle_eddy.mat` matrix [34] exemplifies the advantages and disadvantages of both algorithms. It can be seen in Fig. 5a that the largest 0.01% singular values of `shuttle_eddy.mat` correspond to positive eigenvalues. Alg. 2 gives less error when $k = \frac{n}{100}$ since the leading order singular values correspond to positive eigenvalues. However, Alg. 3 gives less error for larger k since some of the k/n largest singular values correspond to negative eigenvalues.

4 Application of PSD Projections: Semidefinite Least Squares Problems

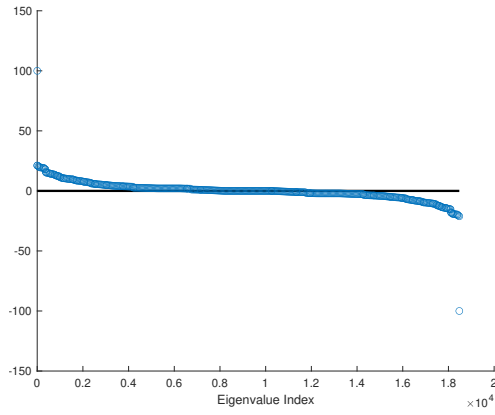
In Section 3 we introduced two randomized algorithms for approximate projecting matrices onto the PSD cone (Algorithms 2 and 3). PSD projections are widely



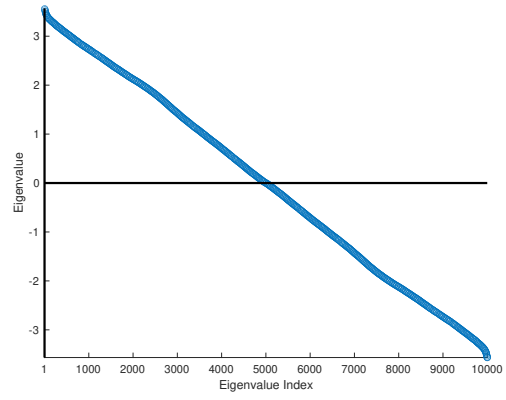
(a) shuttle_eddy.mat



(b) cyl6.mat



(c) lowThrust_13.mat



(d) G67.mat

Figure 5: Scatter plot showing the distribution of the eigenvalues $\lambda_1 \geq \dots \geq \lambda_n$ for various benchmark matrices from [34], whose projections are analysed in Table 1.

used in many first-order semidefinite programming (SDP) solvers. We next recap the first-order solver for solving Semidefinite Programming Least Square (SDLS) problems from [35], showing how to modify this algorithm to solve SDPs and how we can employ our randomized PSD projection algorithms.

Consider the following SDLS problem,

$$\begin{aligned} \min_{X \in \mathbb{S}_n^+} \quad & \frac{1}{2} \left\| X - \frac{1}{\rho} C \right\|_2^2 \\ \text{subject to: } & \text{Tr}(A_i^\top X) = b_i \text{ for } i \in \{1, \dots, m\}, \end{aligned} \quad (36)$$

where $\rho > 0$, $b \in \mathbb{R}^m$, $C \in \mathbb{S}_n$ and $\{A_i\}_{i \in \{1, \dots, m\}} \subset \mathbb{S}_n$ is the problem data, and X the decision variable.

Following the partial dualization approach of [35, 36] and [22] for solving (36). Consider the partial Lagrangian of Opt. (36):

$$L(X; y) := \frac{1}{2} \left\| X - \frac{1}{\rho} C \right\|_2^2 - \sum_{i=1}^m y_i (\text{Tr}(A_i^\top X) - b_i),$$

where only the affine constraint have been pulled into the Lagrangian. The dual problem is thus given by,

$$\sup_{y \in \mathbb{R}^m} \inf_{X \in \mathbb{S}_n^+} L(X; y). \quad (37)$$

Define $X^*(y) := \inf_{X \in \mathbb{S}_n^+} L(X; y)$. The following lemma gives an analytical expression for $X^*(y)$.

Lemma 4. Consider $X^*(y) := \inf_{X \in \mathbb{S}_n^+} L(X; y)$. It follows that

$$X^*(y) = \left(\frac{1}{\rho} C + \sum_{i=1}^m y_i A_i \right)_+. \quad (38)$$

Proof. By completing the square in $L(x; y)$ it follows that,

$$L(X; y) = \frac{1}{2} \left\| X - \frac{1}{\rho} C - \sum_{i=1}^m y_i A_i \right\|_2^2 - y^\top b - \frac{1}{2} \left\| \sum_{i=1}^m y_i A_i \right\|_2^2 - \sum_{i=1}^m \frac{y_i}{\rho} \text{Tr}(A_i^\top C).$$

Only the first term in L involves X . Hence, solving $\inf_{X \in \mathbb{S}_n^+} L(X, y)$ is equivalent to solving $\inf_{X \in \mathbb{S}_n^+} \left\| X - \frac{1}{\rho} C - \sum_{i=1}^m y_i A_i \right\|_2^2$. Therefore by Theorem 1 Eq. (38) holds. Furthermore, note that as A_i and C are symmetric, so is their weighted sum, and hence the projection in solution (38) exists. \square

Now by Lemma 4 the dual problem, given in Eq. (37), is reduced to the following unconstrained optimization problem,

$$\sup_{y \in \mathbb{R}^m} \theta(y) := L(X^*(y), y). \quad (39)$$

It has been previously shown in [35] that Opt. (39) is concave, coercive, and has Lipschitz continuous gradient that is given by

$$\nabla \theta(y) = -(\text{Tr}(A_1^\top X^*(y)) - b_1, \dots, \text{Tr}(A_m^\top X^*(y)) - b_m)^\top.$$

Using a first order method, like Gradient Descent (GD), to solve Opt. (39) necessitates the computation of PSD projections through X^* in Eq. (38). For large scale problems this may be numerically prohibitive. Therefore we next propose computing $\nabla \theta$ by using our proposed randomized projection from Sec. 3. This approach is illustrated in Alg. 6. The expected error of the computation of $\nabla \theta$ through our RNLA PSD projection is given in the following corollary.

Corollary 3 (Randomized gradient error bound). *Let $y \in \mathbb{R}^m$ and consider $X := \left(\frac{1}{\rho}C + \sum_{i=1}^m y_i A_i\right) \in \mathbb{S}_n$, where $C, A_i \in \mathbb{S}_n$, and $\rho > 0$. Choose a target rank $k \geq 2$ and an oversampling parameter $l \geq 2$, where $k + l \leq n$. Execute Algorithm 2 with $q = 0$ to output \hat{X}_+ . Construct an approximation of $\nabla \theta$;*

$$\nabla \hat{\theta}(y) := -(\text{Tr}(A_1^\top \hat{X}_+) - b_1, \dots, \text{Tr}(A_m^\top \hat{X}_+) - b_m)^\top.$$

Then

$$\mathbb{E}[\|\nabla \theta(y) - \nabla \hat{\theta}(y)\|_2] \leq \left(\sum_{i=1}^m \|A_i\|_2\right) (1 + \sqrt{k+l}) \varepsilon_1(\{\sigma_i(X)\}_{i=1}^n, k, l) \quad (40)$$

where the expectation is taken with respect to the randomly generated matrix Ω in Algorithm 1 and the ε_1 term is defined in Eqs (15).

Proof. For convenience, let us denote the Frobenius inner product by $\langle X, Y \rangle_F = \text{Tr}(X^\top Y)$. Now, applying the Cauchy Schwartz inequality and the sub-additivity property of the square root operator we get that

$$\begin{aligned} \|\nabla \theta(y) - \nabla \hat{\theta}(y)\|_2 &= \|\text{Tr}(A_1^\top (\hat{X}_+ - X_+)), \dots, \text{Tr}(A_m^\top (\hat{X}_+ - X_+))\|_2 \\ &= \sqrt{\sum_{i=1}^m \langle A_i, \hat{X}_+ - X_+ \rangle_F^2} \leq \sqrt{\sum_{i=1}^m \|A_i\|_2^2 \|\hat{X}_+ - X_+\|_2^2} \\ &\leq \sum_{i=1}^m \|A_i\|_2 \|\hat{X}_+ - X_+\|_2. \end{aligned}$$

Finally, take expectations and apply Eq. (17). □

By a similar argument to Corollary 3 we can also establish an error bound for using the randomized scaled projection (Algorithm 3) using Proposition 2. We can also derive bounds in terms of the spectral norms for both algorithms using the equivalence between the two norms, $\|\hat{X}_+ - X\|_2 \leq \sqrt{n}\|\hat{X}_+ - X\|_\infty$, and the spectral error bounds in Eqs (18) and (27). These gradient error bounds are required to use the many convergence results for problems with stochastic biased gradient error [23, 24, 25]. We now reformulate Opt. (36) into a more natural form

Algorithm 6 Dual gradient descent to solve Opt. (36).

Input: SDP parameters: $C \in \mathbb{S}_n$, $\rho > 0$, $A_i \in \mathbb{S}_n$, $b \in \mathbb{R}^m$.
RNLA proj parameters: $k, l, q, N \in \mathbb{N}$, $\text{scal} \in \{0, 1\}$.
GD parameters: $\varepsilon > 0$, $\beta > 0$, $M \in \mathbb{N}$.
Output: $X_+ \in \mathbb{S}_n^+$ approximate solution to Opt. (36).

```

1:  $y = \text{randn}(m, 1)$  ▷ Randomized GD initialization
2:  $\nabla\theta(y) = \varepsilon \text{ones}(m, 1)$ ;  $i = 0$  ▷ Gradient initialization
3: while  $\|\nabla\theta(y)\|_2 > \varepsilon$  and  $i \leq M$  do
4:    $i = i + 1$ 
5:    $X = (1/\rho)C + \sum_{i=1}^m y_i A_i$ 
6:   if  $\text{scal}=1$  then
7:      $\alpha = \text{min\_eig}(X, N)$  ▷ Alg. 5
8:      $\hat{X}_+ = \text{ran\_proj\_scal}(X, k, l, q, \alpha)$  ▷ Alg. 3
9:   else
10:     $\hat{X}_+ = \text{ran\_proj}(X, k, l, q)$  ▷ Alg. 2
11:   end if
12:    $\nabla\hat{\theta}(y) = (\text{Tr}(A_1^\top \hat{X}_+), \dots, \text{Tr}(A_m^\top \hat{X}_+))^\top - b$  ▷ Cor. 3
13:    $y = y - \beta \nabla\theta(y)$  ▷ Update GD iteration
14: end while

```

for specifying SDPs. By expanding the squared objective, multiplying through by $\rho > 0$ and removing constant terms in the SDLS problem given in Opt. (36) we arrive at the following equivalent problem,

$$\begin{aligned}
& \min_{X \in \mathbb{S}_n^+} \text{Tr}(\tilde{C}^\top X) + \frac{\rho}{2} \|X\|_2^2 \\
& \text{subject to: } \text{Tr}(A_i^\top X) = b_i \text{ for } i \in \{1, \dots, m\},
\end{aligned} \tag{41}$$

where $\tilde{C} = -C \in \mathbb{S}_n$, which is a standard SDP with Tikhonov regularization.

Degree= 4, SDP size: [n, m] = [3026, 715]	Mosek	eig	k=[0.2n] scal=1	k=[0.1n] scal=1	k=[0.05n] scal=1	k=[0.2n] scal=0	k=[0.1n] scal=0	k=[0.05n] scal=0
Computation time (s)	0.176	1.65	2.1	1.8	1.6	1.8	1.5	1.46
$\sqrt{\sum_{i=1}^m (\text{Tr}(A_i^\top X) - b_i)^2}$	1.75e-9	4.5e-3	0.1	0.15	0.14	2.08	5.5	2.08
$ \gamma - \gamma^* $	6.52e-10	1.54e-5	4.5e-5	1.76e-5	5.1e-5	3.1e-5	9.56e-4	1e-3
Degree= 6, SDP size: [n, m] = [48401, 5005]								
Computation time (s)	8.82	19.26	22.1	17.8	16.9	16.2	11.9	10.7
$\sqrt{\sum_{i=1}^m (\text{Tr}(A_i^\top X) - b_i)^2}$	7e-12	4.5e-2	0.33	0.44	0.43	2.37	2.37	2.33
$ \gamma - \gamma^* $	1.9e-12	2.7e-4	1.25e-4	2.3e-4	1.43e-4	3.53e-4	2.1e-3	9.9e-3
Degree= 8, SDP size: [n, m] = [511226, 24310]								
Computation time (s)	690.6	201	188	156.8	141.7	160.8	134.7	114.6
$\sqrt{\sum_{i=1}^m (\text{Tr}(A_i^\top X) - b_i)^2}$	6.83e-11	0.17	3.37	3.1	3.3	3.73	9.78	9.75
$ \gamma - \gamma^* $	1.1e-11	1.7e-3	1.7e-3	1.6e-3	1.2e-3	1.07e-4	6.4e-3	1.9e-2
Degree= 10, SDP size: [n, m] = [4008005, 92378]								
Computation time (s)	∞	2275.7	2389.9	1992.8	1820.6	2179	1909.5	1734.6
$\sqrt{\sum_{i=1}^m (\text{Tr}(A_i^\top X) - b_i)^2}$	∞	3.5e-2	0.86	0.99	1.2	1.05	5.27	1.05
$ \gamma - \gamma^* $	∞	4.2e-5	1.19e-4	7.5e-5	1.19e-4	4.8e-5	3e-4	1.3e-3

Table 2: Performance of various algorithms for solving the SDP problem associated with Opt. (42). Values of ∞ signify the solver failed to provide a solution due to excessive memory requirements.

5 Numerical Examples

The following numerical examples demonstrate the properties of Algorithm 6. All computation was carried out using an Apple M1 Macbook Pro with 16GB of RAM.

Example 1. Consider an SDLS Problem (36) with two constraints ($m = 2$). We formulate the problem by using Matlab to generate $\tilde{A}_i = \text{randn}(n)$ and making this normalized and symmetric by $A_i = \frac{\tilde{A}_i^\top + \tilde{A}_i}{2\|\tilde{A}_i\|_2}$ for $i \in \{1, 2\}$. To ensure the problem is feasible we randomly generate $X_0 \in \mathbb{S}_n$ and set $b_i = \text{Tr}(A_i^\top X_0)$. Similarly, we randomly generate $C \in \mathbb{S}_n$. The blue diamonds in Fig. 6 show 100 GD iterations of Alg. 6, randomly initiated at $y = [1.2753, 0.2418]^\top$ and executed for $n = 200$, $\rho = 1$, $M = 100$, $\beta = 0.5$, $k = 75$, $l = 10$, $q = 6$, $\text{scal} = 1$. The red stars show the output of Alg. 6 when the full deterministic eigen-decomposition is executed during each iteration of GD. We also plot the level sets of the dual objective function $\theta(y) := L(X^*(y), y)$. The algorithm using the full eigen-decomposition converges to the optimal solution, $y^* = [-0.04 - 1.19]^\top$, while the algorithm using low-rank randomized eigenvalue decompositions converges to a nearby solution. Upon termination, the constraint error, $\sqrt{\sum_{i=1}^2 (\text{Tr}(A_i^\top X) - b_i)^2}$, was

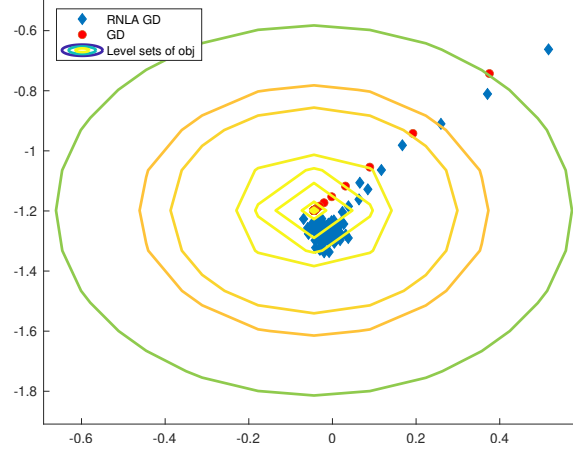


Figure 6: Plot associated with Ex. 1 showing convergence of GD algorithms.

$2.8e-15$ for the deterministic GD and 0.0437 for the RNLA GD output.

Example 2. We now consider the Sum-of-Squares (SOS) relaxation to an unconstrained polynomial optimization problem [37]. The objective is to find a certifiable lower bound on the minimum of a given polynomial $p : \mathbb{R}^n \rightarrow \mathbb{R}$. The SOS relaxation of this is:

$$\gamma^* = \min \gamma \quad \text{subject to } p(x) + \gamma \in \sum_{SOS}, \quad (42)$$

Where \sum_{SOS} denotes the set of sum-of-squares polynomials. One of the main reasons SOS problems are convenient is they can be solved via semidefinite programming [37]. Unfortunately the size of the resulting SDP scales unfavorably with the degree of p . We solved a regularized version of this SDP, given in Eq. (41), using Alg. 6. To test performance we randomly generate p such that the solution to Opt. (42) is analytically known. We set $p(x) = z_d(x)Xz_d(x) - \pi$, where z_d is the vector of d -degree monomial basis functions and $X \in \mathbb{S}_n^+$ is randomly generated. The solution is then $\gamma^* = \pi$.

The number of independent variables in p is fixed to 9 and the degree is varied. Columns $k = 0.2n$, $k = 0.1n$, and $k = 0.05n$ in Table 2 show information about Alg. 6 when the parameters are fixed to $l = 10$, $q = 8$, $M = 4000$, $N = 10$, $\rho = 0.1$, $\beta = 0.01$, $\varepsilon = 1e-10$ and $scal=1$ or 0. Column *eig* shows the results of executing Alg. 6 when the analytical PSD projection is executed during each iteration of GD.

As expected, since Mosek is a second order interior point method it exhibits greater speed and accuracy for smaller problems. However, for large SDPs (degree 10) Mosek fails due to memory requirements. The first order method of Alg. 6 is still able to output $\gamma^ = \pi$ to 3dp even when $k = \lceil 0.05n \rceil$. Across the board we see better performance when using $\text{scal} = 1$.*

6 Conclusion

We have proposed a highly scalable method of harnessing RNLA to compute approximate PSD projections. We’ve shown that in some cases it is advantageous to scale the matrix to align the largest singular values with the largest positive eigenvalues before approximating by a low rank matrix and projecting. Furthermore we have implemented our approximate projection methods into a first order SDP solver, demonstrating the potential of using RNLA projections for solving large scale SDP and SOS problems. In future work we will explore replacing Alg. 1 with the adaptive rank revealing algorithms of [38, 39].

Acknowledgement

The first author would like to thank and the Dr Jeff Wadsworth – Battelle Knowledge Exchange Scheme Award, the University of Sheffield and Columbia University for supporting a summer visit that resulted in a collaboration and the production of this work. The second author would like to acknowledge funding from the National Science Foundation under grant ECCS 2144634.

References

- [1] A. Yurtsever, J. A. Tropp, O. Fercoq, M. Udell, and V. Cevher, “Scalable semidefinite programming,” *SIAM Journal on Mathematics of Data Science*, vol. 3, no. 1, pp. 171–200, 2021.
- [2] N. J. Higham, “Computing the nearest correlation matrix—a problem from finance,” *IMA journal of Numerical Analysis*, vol. 22, no. 3, pp. 329–343, 2002.

- [3] I. Banno, S.-I. Azuma, R. Ariizumi, T. Asai, and J.-I. Imura, “Data informativity for lyapunov equations,” *IEEE Control Systems Letters*, vol. 7, pp. 2365–2370, 2023.
- [4] W. C. Thacker, “The role of the hessian matrix in fitting models to measurements,” *Journal of Geophysical Research: Oceans*, vol. 94, no. C5, pp. 6177–6196, 1989.
- [5] N. J. Higham, “Computing a nearest symmetric positive semidefinite matrix,” *Linear algebra and its applications*, vol. 103, 1988.
- [6] L. Vandenberghe, V. R. Balakrishnan, R. Wallin, A. Hansson, and T. Roh, “Interior-point algorithms for semidefinite programming problems derived from the kyp lemma,” *Positive polynomials in control*, pp. 195–238, 2005.
- [7] B. O’donoghue, E. Chu, N. Parikh, and S. Boyd, “Conic optimization via operator splitting and homogeneous self-dual embedding,” *Journal of Optimization Theory and Applications*, vol. 169, 2016.
- [8] L. Yang, D. Sun, and K.-C. Toh, “SDPNAL+: a majorized semismooth Newton-CG augmented lagrangian method for semidefinite programming with nonnegative constraints,” *Mathematical Programming Computation*, vol. 7, no. 3, pp. 331–366, 2015.
- [9] Y. Zheng, G. Fantuzzi, A. Papachristodoulou, P. Goulart, and A. Wynn, “Chordal decomposition in operator-splitting methods for sparse semidefinite programs,” *Mathematical Programming*, vol. 180, 2020.
- [10] Y. Zheng, G. Fantuzzi, and A. Papachristodoulou, “Exploiting sparsity in the coefficient matching conditions in sum-of-squares programming using ADMM,” *IEEE control systems letters*, 2017.
- [11] N. Rontsis, P. Goulart, and Y. Nakatsukasa, “Efficient semidefinite programming with approximate ADMM,” *Journal of Optimization Theory and Applications*, pp. 1–29, 2022.
- [12] J. B. Francisco and D. S. Goncalves, “A fixed-point method for approximate projection onto the positive semidefinite cone,” *Linear Algebra and its Applications*, vol. 523, pp. 59–78, 2017.

- [13] N. Halko, P.-G. Martinsson, and J. A. Tropp, “Finding structure with randomness: Probabilistic algorithms for constructing approximate matrix decompositions,” *SIAM review*, vol. 53, pp. 217–288, 2011.
- [14] M. Udell and A. Townsend, “Why are big data matrices approximately low rank?,” *SIAM Journal on Mathematics of Data Science*, vol. 1, no. 1, pp. 144–160, 2019.
- [15] J. Yuan and A. Lamperski, “A random algorithm for semidefinite programming problems,” in *2018 Annual American Control Conference (ACC)*, pp. 1382–1387, IEEE, 2018.
- [16] M. Guedes-Ayala, P.-L. Poirion, L. Schewe, and A. Takeda, “Sparse subgaussian random projections for semidefinite programming relaxations,” *arXiv preprint arXiv:2406.14249*, 2024.
- [17] H. Fawzi and H. Goulbourne, “Faster proximal algorithms for matrix optimization using jacobi-based eigenvalue methods,” *Advances in Neural Information Processing Systems*, vol. 34, 2021.
- [18] M. Souto, J. D. Garcia, and Á. Veiga, “Exploiting low-rank structure in semidefinite programming by approximate operator splitting,” *Optimization*, vol. 71, no. 1, pp. 117–144, 2022.
- [19] S. D. Bopardikar, “Randomized matrix factorization for Kalman filtering,” in *2017 American Control Conference (ACC)*, IEEE, 2017.
- [20] H. Wang and J. Anderson, “Large-scale system identification using a randomized SVD,” in *2022 American Control Conference (ACC)*, pp. 2178–2185, IEEE, 2022.
- [21] H. Wang and J. Anderson, “Learning linear models using distributed iterative hessian sketching,” in *Learning for Dynamics and Control Conference*, pp. 427–440, PMLR, 2022.
- [22] D. Henrion and J. Malick, “Projection methods for conic feasibility problems: applications to polynomial sum-of-squares decompositions,” *Optimization Methods & Software*, vol. 26, no. 1, pp. 23–46, 2011.
- [23] J. Chen and R. Luss, “Stochastic gradient descent with biased but consistent gradient estimators,” *arXiv preprint arXiv:1807.11880*, 2018.

- [24] Y. Hu, S. Zhang, X. Chen, and N. He, “Biased stochastic gradient descent for conditional stochastic optimization,” *arXiv preprint arXiv:2002.10790*, 2020.
- [25] K. Scaman and C. Malherbe, “Robustness analysis of non-convex stochastic gradient descent using biased expectations,” *Advances in Neural Information Processing Systems*, vol. 33, 2020.
- [26] N. J. Higham, “Stable iterations for the matrix square root,” *Numerical Algorithms*, vol. 15, pp. 227–242, 1997.
- [27] S. Boyd and L. Vandenberghe, *Convex optimization*. Cambridge university press, 2004.
- [28] P.-G. Martinsson, A. Szlam, M. Tygert, *et al.*, “Normalized power iterations for the computation of svd,” *Manuscript.*, Nov, 2010.
- [29] J.-B. Hiriart-Urruty and C. Lemaréchal, *Fundamentals of convex analysis*. Springer Science & Business Media, 2004.
- [30] R. Bhatia, “Modulus of continuity of the matrix absolute value,” *Indian Journal of Pure and Applied Mathematics*, vol. 41, pp. 99–111, 2010.
- [31] R. T. Powers and E. Størmer, “Free states of the canonical anticommutation relations,” *Communications in Mathematical Physics*, 1970.
- [32] R. Mises and H. Pollaczek-Geiringer, “Praktische verfahren der gleichungsauflösung,” *ZAMM-Journal of Applied Mathematics and Mechanics/Zeitschrift für Angewandte Mathematik und Mechanik*, vol. 9, no. 1, pp. 58–77, 1929.
- [33] Z.-Z. Bai, W.-T. Wu, and G. V. Muratova, “The power method and beyond,” *Applied Numerical Mathematics*, vol. 164, pp. 29–42, 2021.
- [34] T. A. Davis and Y. Hu, “The University of Florida sparse matrix collection,” *ACM Transactions on Mathematical Software (TOMS)*, vol. 38, no. 1, pp. 1–25, 2011.
- [35] J. Malick, “A dual approach to semidefinite least-squares problems,” *SIAM Journal on Matrix Analysis and Applications*, 2004.

- [36] J. Malick, J. Povh, F. Rendl, and A. Wiegele, “Regularization methods for semidefinite programming,” *SIAM Journal on Optimization*, vol. 20, no. 1, pp. 336–356, 2009.
- [37] P. A. Parrilo, “Semidefinite programming relaxations for semialgebraic problems,” *Mathematical programming*, vol. 96, pp. 293–320, 2003.
- [38] P.-G. Martinsson and S. Voronin, “A randomized blocked algorithm for efficiently computing rank-revealing factorizations of matrices,” *SIAM Journal on Scientific Computing*, vol. 38, no. 5, pp. S485–S507, 2016.
- [39] W. Yu, Y. Gu, and Y. Li, “Efficient randomized algorithms for the fixed-precision low-rank matrix approximation,” *SIAM Journal on Matrix Analysis and Applications*, vol. 39, no. 3, pp. 1339–1359, 2018.
- [40] H. Araki, “On quasifree states of CAR and Bogoliubov automorphisms,” *Publications of the Research Institute for Mathematical Sciences*, 1971.
- [41] T. Kato, “Continuity of the map $S \rightarrow |S|$ for linear operators,” *Proceedings of the Japan Academy*, vol. 49, no. 3, pp. 157–160, 1973.

7 Appendix

Lemma 5 (An Inequality for the Frobenius norm). *Suppose $A, B \in \mathbb{S}_n$ then*

$$\left\| (A^\top A)^{\frac{1}{2}} - (B^\top B)^{\frac{1}{2}} \right\|_2 \leq \|A - B\|_2. \quad (43)$$

Proof. In finite dimensions the Hilbert-Schmidt operator is identical to the Frobenius norm and hence Eq. (43) follows by Lemma 5.2 in [40]. \square

Lemma 6 (An Inequality for the spectral norm [41]). *Suppose $A, B \in \mathbb{S}_n$ then*

$$\left\| (A^\top A)^{\frac{1}{2}} - (B^\top B)^{\frac{1}{2}} \right\|_\infty \leq \frac{2}{\pi} \left(2 + \log \left(\frac{\|A\|_\infty + \|B\|_\infty}{\|A - B\|_\infty} \right) \right) \|A - B\|_\infty. \quad (44)$$

Theorem 2 ([13]). *Consider $A \in \mathbb{R}^{m \times n}$. Choose a target rank $k \geq 2$ and an oversampling parameter $l \geq 2$, where $k + l \leq \min\{m, n\}$. Execute the Randomized Range Finder (Algorithm 1) for $q \in \mathbb{N}$ to output an orthonormal approximate basis Q which satisfies,*

$$\begin{aligned} & \mathbb{E}[\|A - QQ^\top A\|_\infty] \\ & \leq \left(1 + \sqrt{\frac{k}{l-1}} + \frac{e\sqrt{k+l}}{l} \sqrt{\min\{m, n\} - k}\right)^{\frac{1}{2q+1}} \sigma_{k+1}(A), \end{aligned} \quad (45)$$

where the expectation is taken with respect to the randomly generated matrix Ω .

Moreover when the Randomized Range Finder (Algorithm 1) is executed with $q = 0$ then the following bound in the Frobenius norm is satisfied,

$$\mathbb{E}[\|A - QQ^\top A\|_2] \leq \sqrt{\left(1 + \frac{k}{l-1}\right) \left(\sum_{j>k} \sigma_j(A)^2\right)}. \quad (46)$$

Lemma 7. For any $x \geq 0$ we have

$$\log(x) \leq \frac{1}{2}\sqrt{x} \quad \text{and} \quad (47)$$

$$-x \log(x) \leq \min\{\sqrt{x}, e^{-1}\}. \quad (48)$$

Proof. Let $g(x) = \log(x) - 0.5\sqrt{x}$. To show Eq. (47) we show $\sup_{x \geq 0} g(x) \leq 0$. To find the max point of g we find it's stationary points, $g'(x) = \frac{1}{x} - \frac{1}{4\sqrt{x}} = \frac{4-\sqrt{x}}{4\sqrt{x}}$. Clearly $g'(16) = 0$. Moreover, $g''(x) = -\frac{1}{x^2} + \frac{1}{8x^{3/2}} = \frac{\sqrt{x}-8}{8x^2}$ and hence $g''(16) = \frac{-4}{8(16)^2} < 0$ implying this stationary point is a max point. Therefore, $\sup_{x \geq 0} g(x) = g(16) = \log(16) - 2 = -0.796 < 0$.

Let $f(x) := -x \log(x) - \sqrt{x}$. To show Eq. (48) we show $f(0) = 0$ and $f'(x) < 0$, that is f is monotonically decreasing and hence $0 = f(0) \geq f(x)$. To show $f(0) = 0$ note that $\sqrt{0} = 0$ and $x \log(x)$ is continuous with $\lim_{x \rightarrow 0} x \log(x) = 0$ can be shown by L'Hôpital's rule. Now, $f'(x) = -\log(x) - 1 - \frac{1}{2\sqrt{x}}$. Clearly, when $x > 1$ we have $\log(x) > 0$ and hence each of the terms in $f'(x)$ are negative implying $f'(x)$ is negative when $x > 1$. We next show $f'(x) < 0$ when $x \in [0, 1]$ which is equivalent to showing $f'(1/y) = \log(y) - 1 - (1/2)\sqrt{y}$ is negative for $y \geq 1$. By Eq. (47) we have that $f'(1/y) = \log(y) - (1/2)\sqrt{y} - 1 \leq -1 < 0$ and hence $-x \log(x) < \sqrt{x}$. On the other hand the maximum of $h(x) := -x \log(x)$ occurs when $h'(x) = -\log(x) - 1 = 0$ which is solved at $x = 1/e$. Moreover, $h''(1/e) = -\frac{1}{1/e} = -e < 0$ implying this is a max point. Hence $-x \log(x) < h(1/e) = e^{-1}$. \square

Lemma 8. Consider any $X \in \mathbb{S}_k$. Suppose $Q \in \mathbb{R}^{n \times k}$ is such that $Q^\top Q = I$. Then

$$QX_+Q^\top = (QXQ^\top)_+ \quad (49)$$

Proof.

$$QX_+Q^\top \stackrel{(13)}{=} \frac{1}{2}Q(X + \sqrt{X^\top X})Q^\top = \frac{1}{2}(QXQ^\top + Q\sqrt{X^\top X}Q^\top). \quad (50)$$

We next show $Q\sqrt{X^\top X}Q^\top = \sqrt{QX^\top XQ^\top}$. First note that $Q\sqrt{X^\top X}Q^\top \in S_n^+$ by definition that $\sqrt{X^\top X} \in \mathbb{S}_n^+$ is the uniquely defined square root of $X^\top X$ (see notation section). Next, note that it follows from $Q^\top Q = I$ that

$$Q\sqrt{X^\top X}Q^\top Q\sqrt{X^\top X}Q^\top = Q\sqrt{X^\top X}\sqrt{X^\top X}Q^\top = QX^\top XQ^\top.$$

Since the square root of $QX^\top XQ^\top$ is uniquely defined it follows that $\sqrt{QX^\top XQ^\top} = Q\sqrt{X^\top X}Q^\top$. Upon substituting into Eq. (50) and using $Q^\top Q = I$ again, we deduce that

$$\begin{aligned} QX_+Q^\top &\stackrel{(50)}{=} \frac{1}{2}(QXQ^\top + Q\sqrt{X^\top X}Q^\top) = \frac{1}{2}(QXQ^\top + \sqrt{QX^\top XQ^\top}) \\ &= \frac{1}{2}(QXQ^\top + \sqrt{QX^\top Q^\top QXQ^\top}) \stackrel{(13)}{=} (QXQ^\top)_+. \end{aligned}$$

□

Lemma 9. Consider $X \in \mathbb{S}_n$. It follows that $|\lambda_n(X)| := |\min_i \lambda_i(X)| = |\sigma_1(Y) - \sigma_1(X)|$, where $Y := X - \sigma_1(X)I$.

Proof. Since $X \in \mathbb{S}_n$ is a symmetric matrix it has the property that the absolute values of their eigenvalues are exactly equal to their singular values, i.e., $\{|\lambda_1(X)|, \dots, |\lambda_n(X)|\} = \{\sigma_1(X), \dots, \sigma_n(X)\}$. It follows that $Y \in \mathbb{S}_n$ is simultaneously diagonalize with X with eigenvalues shifted by negative $\sigma_1(X)$. That is, $\lambda_i(Y) = \lambda_i(X) - \sigma_1(X) = \lambda_i(X) - \max_i |\lambda_i(X)| < 0$ and hence $\sigma_i(Y) = |\lambda_{n-i+1}(X) - \sigma_1(X)|$. There are two possible cases depending if the largest singular value of X corresponds to the absolute value of the maximal or minimal eigenvalue of X :

- **Case 1:** $\sigma_1(X) = |\lambda_n(X)|$

This implies that the absolute value of the minimal eigenvalue is greater than the absolute value of the maximum eigenvalue of X , $|\lambda_n(X)| \geq |\lambda_1(X)|$. Then it follows that the minimal eigenvalue of X must be negative, $\lambda_n(X) \leq 0$, otherwise if $0 \leq \lambda_n(X) \leq \lambda_1(X)$ we would contradict $|\lambda_n(X)| \geq |\lambda_1(X)|$. Now $\sigma_1(Y) = |\lambda_n(X) - \sigma_1(X)| = |\lambda_n(X) - |\lambda_n(X)|| = 2|\lambda_n(X)|$. Hence $|\sigma_1(Y) - \sigma_1(X)| = |(2|\lambda_n(X)| - |\lambda_n(X)|)| = |\lambda_n(X)|$.

- **Case 2:** $\sigma_1(X) = |\lambda_1(X)|$

By a similar argument to Case 1 we get $\lambda_1(X) \geq 0$ and hence $\sigma_1(X) = \lambda_1(X)$. Moreover since $\lambda_1(X) \geq \lambda_n(X)$ we get that $\sigma_1(Y) = \lambda_1(X) - \lambda_n(X)$. Hence, $|\sigma_1(Y) - \sigma_1(X)| = |\lambda_1(X) - \lambda_n(X) - \sigma_1(X)| = |\lambda_n(X)|$.

□